Comparison of Biodiesel Performance Based on HCCI Engine Simulation Using Detailed Mechanism with On-the-fly Reduction

ARTICLE *in* ENERGY & FUELS · FEBRUARY 2012

Impact Factor: 2.79 · DOI: 10.1021/ef2019512

4 AUTHORS, INCLUDING:

Shuliang Zhang
Rutgers, The State University of New Jersey
6 PUBLICATIONS **28** CITATIONS
SEE PROFILE

Ioannis Androulakis
Rutgers, The State University of New Jersey
198 PUBLICATIONS **2,855** CITATIONS
SEE PROFILE

Marianthi Ierapetritou
Rutgers, The State University of New Jersey
143 PUBLICATIONS **1,582** CITATIONS
SEE PROFILE

energy&fuels

Article

pubs.acs.org/EF

Comparison of Biodiesel Performance Based on HCCI Engine Simulation Using Detailed Mechanism with On-the-fly Reduction

Shuliang Zhang,[†] Linda J. Broadbelt,[‡] Ioannis P. Androulakis,[†] and Marianthi G. Ierapetritou[†,*]

[†]Department of Chemical and Biochemical Engineering, Rutgers, The State University of New Jersey, Piscataway, New Jersey 08854

[‡]Department of Chemical and Biological Engineering, Northwestern University, Evanston, Illinois 60208

ABSTRACT: Biodiesel is a complex mixture of long-chain methyl esters. Accurate numerical study of biodiesel combustion requires detailed chemistry of large biodiesel surrogates representing realistic biodiesel fuels. However, the detailed kinetic mechanisms for large biodiesel surrogates involve large number of species and reactions, leading to extremely expensive or even infeasible computation when incorporated in engine CFD (computational fluid dynamics) calculations. In this study, the scheme of on-the-fly mechanism reduction incorporated with engine CFD code KIVA-3V is first extended to two large biodiesel surrogate mechanisms, namely methyl decanoate and methyl-9-decenoate. Detailed combustion and engine performance characterization for biodiesel fuels are enabled, and the computational intensity is significantly reduced with satisfactory accuracy. In the simulations, lower CO and NO emissions and lower engine power are observed for biodiesel surrogates. Combustion features such as early oxidation of ester groups are also well captured. This work provides the insight to study combustion and engine operation of complex fuels on the basis of detailed chemistry with efficient mechanism reduction technique.

INTRODUCTION

Facing the burgeoning global energy demands and limited resource of fossil fuels in the world, biodiesel is becoming an important alternative fuel.[1−3] The production and consumption of biodiesel is quickly increasing. With an oxygenated molecular structure, biodiesel has the potential to reduce pollutant emissions. Also, biodiesel can be used with existing diesel engines without major changes. Most importantly, biodiesel is derived from various biorenewable feedstocks, making it promising as an ideal sustainable source of energy. Biodiesel is a complex mixture of monoalkyl esters of long-chain fatty acids derived from a variety of biorenewable sources, such as vegetable oils and animal fats.[4] The most commonly used biodiesel fuels, derived from soybean or rapeseed oil, are mainly composed of five methyl esters including methyl palmitate ($C_{17}H_{34}O_2$), methyl stearate ($C_{19}H_{38}O_2$), methyl oleate ($C_{19}H_{36}O_2$), methyl linoleate ($C_{19}H_{34}O_2$), and methyl linolenate ($C_{19}H_{32}O_2$).[5] These components have similar structures of a methyl ester group attached to a long saturate or unsaturated hydrocarbon chain. The oxygen content in biodiesel could change the combustion features and also contribute to a lower heating value compared to conventional diesel. Also, different physical properties (such as viscosity and volatility) of biodiesel also lead to different fuel spray and mixing process.[6,7] Therefore, biodiesel combustion process has some different characteristics compared with the combustion of conventional diesel fuels.

There are substantial efforts toward understanding the performance of biodiesel combustion. A large number of experimental studies have been focusing on the performance and emissions of biodiesel fuels working with existing diesel engines.[8] Some important characteristics of biodiesel and its combustion process have been investigated. In general, most studies reported lower engine power for biodiesel due to its lower heating value. However, the higher cetane number for biodiesel, that is, advanced ignition, could counterbalance the effect of low heating value and results in similar power in diesel engine.[9] In terms of emission characteristics, it is believed that biodiesel combustion generates less CO, hydrocarbon, and particulate emissions as a result of its oxygenated moiety. Also, for the NO_x emissions, most studies reported increases for biodiesel as a result of the advanced ignition. Lee et al.[9] reported that NO_x emission of biodiesel blend increases about 20% compared to conventional diesel. However, different effects, such as similar or lower NO_x emission, do exist under different engine conditions, as found in the study of Brakora et al.[10]

Although extensive efforts have been made, uncertainties in the biodiesel combustion studies still remain since both physical properties and chemical kinetics affect the overall performance under diesel engine conditions. The combustion kinetics of biodiesel is still not fully understood because detailed information in the combustion process is not easy to capture through experiments. Therefore, computational study of biodiesel combustion is of great interest in order to better explore the underlying details of the biodiesel combustion process. To study the chemical kinetic characteristics of biodiesel, homogeneous charge compression ignition (HCCI) engines are appropriate because the homogeneous engine charge eliminates the effects of mixing related to fuel physical properties.[4]

In HCCI engine simulations, detailed chemical kinetic models of biodiesel surrogates are required to represent the chemistry of biodiesel combustion. In the past few years, chemical kinetic models for various biodiesel surrogates have been developed[11] to facilitate computational study of biodiesel combustion. The first methyl ester kinetic model, proposed by Fisher et al.,[12] is methyl butanoate (MB, $C_5H_{10}O_2$), which is

Received: December 12, 2011
Revised: January 13, 2012
Published: January 16, 2012

   dx.doi.org/10.1021/ef2019512 | *Energy Fuels* 2012, 26, 976−983

relatively small in size compared to the realistic biodiesel components. Um et al.[13] have used this mechanism to study the combustion and emission characteristics in HCCI engine simulations. Detailed kinetic mechanisms for more complex biodiesel surrogates, such as methyl decanoate (MD, $C_{11}H_{22}O_2$), methyl-5-decenoate (MD5D, $C_{11}H_{20}O_2$), and methyl-9-decenoate (MD9D, $C_{11}H_{20}O_2$) have been developed by Herbinet et al.[5,14] These large mechanisms are considered to be better surrogate mechanisms for biodiesel combustion. Most recently, kinetic models for real biodiesel components such as methyl stearate and methyl oleate have also been reported.[15] However, these large mechanisms usually consist of more than 3000 species and around 10000 reactions, and thus cannot be used for reactive flow simulations.

To reduce the computational intensity, many mechanism reduction techniques have been proposed.[16] One category of mechanism reduction approaches is global reduction, including optimization based approaches[17−19] and sensitivity analysis,[20,21] lumping,[22] and the time-integrated flux graph approach.[23] These methods derive a skeletal mechanism that is used throughout the simulation. However, the skeletal mechanism may not be valid for the entire simulation under wide-ranging reaction conditions. To take into account the local conditions, some adaptive reduction approaches have been proposed. *In situ* adaptive tabulations (ISAT),[24] mathematical programming approaches,[25] and graph-based reduction approaches[25−27] belong to this category. The adaptive reduction improves the validity under different conditions, but they rely on the libraries of reduced mechanisms that are developed with priori analysis and simulations. Another category of strategies is based on time scale analysis and quasi-steady-state approximation (QSSA)[28] techniques, such as augmented reduced mechanism (ARM) generation,[29] intrinsic low dimensional manifolds (ILDM),[30] computational singular perturbation (CSP),[31,32] and reaction lumping[33] methods. These approaches identify the fast species with short time scales and separate them by applying QSSA, so that the ODEs describing them are replaced by algebraic equations. In our previous work, an on-the-fly reduction scheme[34] was proposed on the basis of the element flux analysis.[23,35] The on-the-fly reduction calculates a pairwise instantaneous element flux pointer to represent the chemistry transitions under the current conditions in the system, and species pairs with element flux smaller than a user-defined cutoff are excluded in the reduced mechanism. The locally accurate reduced mechanisms are developed dynamically (on-the-fly) according to the specific local conditions, and no *a priori* information of the system is needed. This approach enables us to couple the detailed chemistry with complex reactive flow models such as multidimensional CFD (computational fluid dynamics) scheme with greatly reduced computational costs, while still maintaining satisfactory accuracy.

As we have mentioned, homogeneous charge in HCCI engines eliminates the effect of fuel physical properties on the in-cylinder fuel-air mixing. Therefore, the combustion process is primarily dominated by the chemical kinetics; thus, detailed mechanisms are essential for the computational study of HCCI engine combustion. In this work, two detailed mechanisms for large biodiesel surrogates, namely, methyl decanoate (MD, 2878 species and 8555 reactions) and methyl-9-decenoate (MD9D, 3298 species and 10753 reactions), are incorporated for the first time in the multidimensional CFD simulation of an HCCI engine with on-the-fly reduction approach. Two smaller mechanisms, including a conventional hydrocarbon fuel surrogate *n*-heptane[36] and a small biodiesel surrogate methyl butanoate (MB), are also used for comparison between different types of fuels. The combustion characteristics, emission features, and the engine performance parameters are evaluated and compared among these fuels. To capture NO_x formations, NO_x chemistry is introduced and a multielement flux analysis approach is employed in the on-the-fly reduction to identify fuel oxidation network and NO_x formation network separately. KIVA-3V[37] code is used as the CFD platform, and CHEMKIN[38] is used to handle the chemistry calculation.

PROPOSED SIMULATION FRAMEWORK

A two-dimensional axial symmetric mesh (Figure 1) with 1052 computational cells at bottom dead center (BDC) is employed in KIVA-3V to simulate HCCI engine combustion. The on-the-fly reduction is integrated with KIVA-3V and CHEMKIN code to generate locally accurate reduced mechanism for each computational cell during each time step,[39] and DVODE is applied to numerically solve the resulting ODE system based on each reduced mechanism.

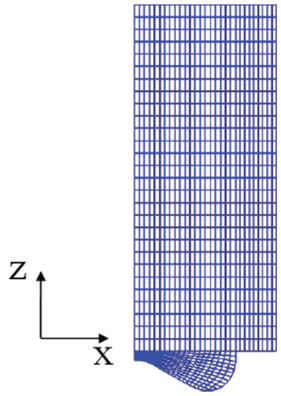

Figure 1. Two-dimensional computational mesh used in KIVA.

In our previous work, we have demonstrated how we determine active species and reactions based on the element flux analysis in the on-the-fly reduction scheme.[23,34] Here, just the main steps are described for the completeness of the presentation. The instantaneous element flux of atom A from species j to species k through reaction i is defined as $\dot{A}_{i,jk}$ by eq 1. The total instantaneous flux from species j to species k through all the reactions involving these species is given by eq 2.

$$\dot{A}_{i,jk}(t) = q_i(t)\frac{n_{A,j}n_{A,k}}{N_{A,i}} \tag{1}$$

$$\overline{A}_{jk}(t) = \sum_{i=1}^{N_R} \dot{A}_{i,jk}(t) \tag{2}$$

where $q_i(t)$ is the instantaneous rate of reaction i (mol/s), $n_{A,j}$ and $n_{A,k}$ are the number of atoms A in species j and k, respectively, $N_{A,i}$ is the total number of atoms A in reaction i, and N_R is the number of reactions in which species j and k participate as reactant or products. However, as shown in our previous study,[34] the calculation of element flux based on the net reaction rate leads to inappropriate representation of element transition involving quasi-steady-state species in partial-equilibrium reactions. This is due to the fact that the net reaction rates of partial-equilibrium reactions are much smaller compared with the forward and reverse reaction rates, so that the element flux

dx.doi.org/10.1021/ef2019512 | *Energy Fuels* 2012, 26, 976−983

computed by eq 1 is relatively small, although fast chemical transition is occurring between the species in both directions. To take into account the effects of these partial-equilibrium reactions, the element flux calculation is modified as eq 3 to include both forward and reverse reaction rates, instead of the net reaction rates.

$$\dot{A}_{i,jk}(t) = (|q_{i,\mathrm{fwd}}(t)| + |q_{i,\mathrm{rev}}(t)|)\frac{n_{A,j}n_{A,k}}{N_{A,i}} \quad (3)$$

where $q_{i,\mathrm{fwd}}(t)$ and $q_{i,\mathrm{rev}}(t)$ are the reaction rates of forward and reverse reactions, respectively.

To capture NO_x emission features of different fuels, NO_x chemistry is incorporated with the oxidation mechanism of each fuel and multielement flux analysis is performed to include both C-element flux and N-element flux. However, as shown in our previous study,[40] N-element flux usually has much smaller value relative to C-element flux. Therefore, N-bearing species are always excluded from the reduced mechanism if both element fluxes are sorted together. To avoid this problem, fluxes based on different elements are calculated and sorted separately. The reduced fuel oxidation network based on C-element flux and the reduced NO_x formation network based on N-element flux are then combined to form the whole set of reduced mechanisms.

In each computational cell and each time step in the CFD calculation, element fluxes are computed for all the source-sink pairs and sorted in descending order. A user-defined cutoff is then applied to identify active species, as well as their involving reactions, that will be included in the reduced mechanism, while species determined inactive are considered dormant and maintain unchanged concentration within the current step. The reduced mechanism is then used in CHEMKIN and DVODE to update species composition, heat release, and temperature profiles, which are passed to KIVA-3V code to formulate fluid mechanics and convection/diffusion process. The integration of on-the-fly convection and KIVA-3V code is illustrated in Figure 2.

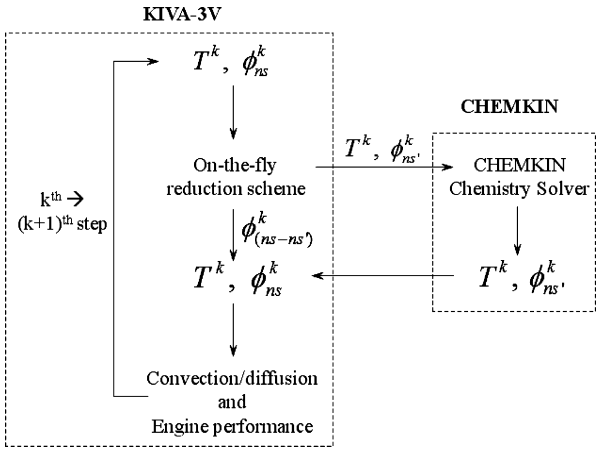

Figure 2. Computational procedures integrating on-the-fly reduction in KIVA-3V.

In addition, to compare the engine performance of different fuels, work done per cycle and engine power output are integrated in KIVA-3V code. Work done by the engine during one engine cycle is approximated by integrating the pressure−volume curve according to eq 4. Power output is defined as the work done per unit time during the entire engine cycles in eq 5, where N is engine speed (rpm) and 2 in the denominator represents the four-stroke engine cycle.[41]

$$W = \int_{\mathrm{cycle}} p\ \mathrm{d}V \quad (4)$$

$$P = \frac{WN}{2} \quad (5)$$

The engine simulations run from crank angle (CA) −30.0° after top dead center (ATDC) to 30.0° ATDC. For each fuel considered in this study, four different engine speeds are used to investigate the combustion and engine performance under different operation conditions. The engine parameters and operation conditions used in the simulations are summarized in Table 1. At lower or higher equivalence ratios, it is possible that the emission levels of CO or NO_x are relatively small, so that the difference between fuels is not obvious. Therefore, we choose to perform our study using equivalence ratio 1.0 at chemical stoichiometry, so we can make better comparisons of the chemical characteristics between fuels.

Table 1. Engine Operation Conditions and Parameters

param.	value
engine speed/rpm	900, 1200, 1500, 1800
initial temp./K	1000
initial pressure/MPa	10
crank angle range/ATCD	−30∼30°
equivalence ratio	1.0
compression ratio	16:1

RESULTS AND DISCUSSION

Framework Validation. To validate the performance of on-the-fly reduction approach, we should compare the on-the-fly reduction results with the detailed mechanism simulation. However, for the two large biodiesel surrogates MD and MD9D, KIVA simulation with detailed mechanisms without using on-the-fly reduction is not feasible because of the extremely long CPU time. In this study, we first validate the on-the-fly reduction with the large mechanisms in Plug Flow Reactor (PFR) simulation. This allows us to select the appropriate cutoff to obtain the necessary accuracy. Then we use the smaller biodiesel surrogate mechanism MB with on-the-fly reduction in KIVA to verify the performance of the integration of on-the-fly reduction in KIVA engine simulations. Finally, we extend the validated KIVA/on-the-fly reduction scheme to the two large biodiesel surrogate mechanisms.

In the PFR simulation, the autoignition delay of MD and MD9D with different initial temperatures is characterized as shown in Figure 3. Stoichiometric fuel/air mixture is used for all the simulations in order to be consistent with engine simulations. The initial temperature ranges from 650 K to 1100 K to cover low-temperature, negative temperature coefficient (NTC), and high-temperature regions. The ignition delay time obtained using on-the-fly reduction is in good agreement with the ignition delay calculated with detailed mechanism. A 99% cutoff used in the on-the-fly reduction is sufficient to produce accurate results. In addition, the predicted ignition delay time of MD is also consistent with shock tube ignition data simulated at the same pressure (12.0 atm) reported by Herbinet et al.,[14] which also provides a validation of the on-the-fly reduction for the two large mechanisms in the simulations. KIVA simulations with

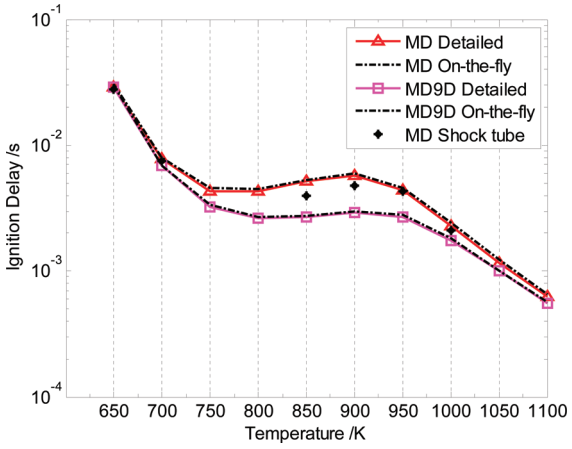

Figure 3. Ignition delay time validation for methyl decanoate and methyl-9-decenoate in PFR simulations. Shock tube ignition data is obtained from Herbinet et al.[14]

MB mechanism using on-the-fly reduction are compared with the simulations with detailed mechanism. In Figure 4, it is

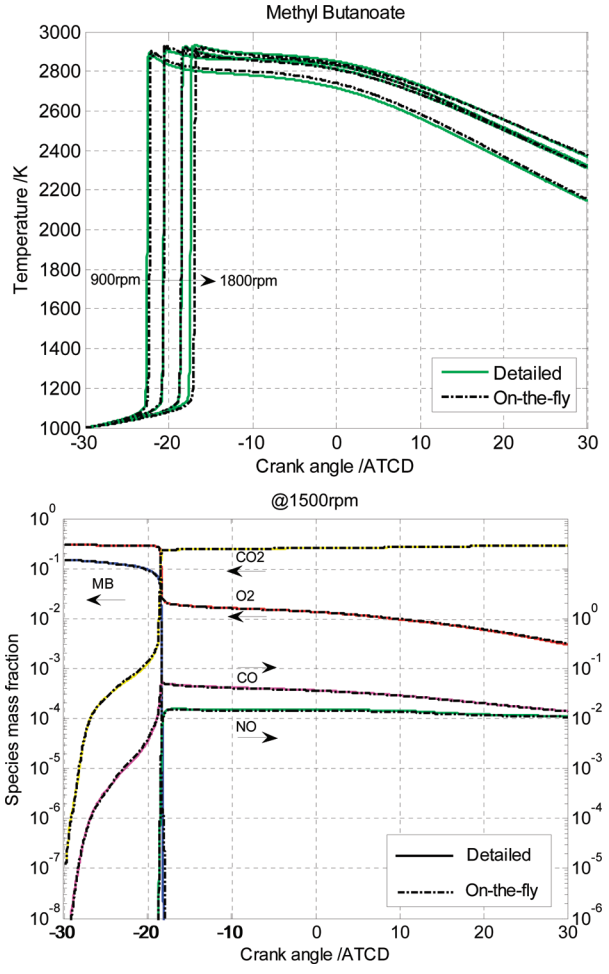

Figure 4. Temperature and selected species profiles in KIVA simulations with methyl butanoate.

shown that the temperature profiles and selected important species profiles calculated using on-the-fly reduction and detailed mechanisms are identical for different engine operation conditions, indicating that the integration of on-the-fly reduction in KIVA can produce reliable simulation results. On the basis of the above validation, we then extend the same KIVA/on-the-fly reduction framework to the two large mechanisms, which finally enable us to conduct engine simulations in KIVA with complex biodiesel surrogate mechanisms while maintaining acceptable computational time and accuracy.

The CPU time of KIVA simulations with on-the-fly reduction is dramatically reduced in our study, especially for the two large mechanisms. As shown in Figure 5, the simulation time

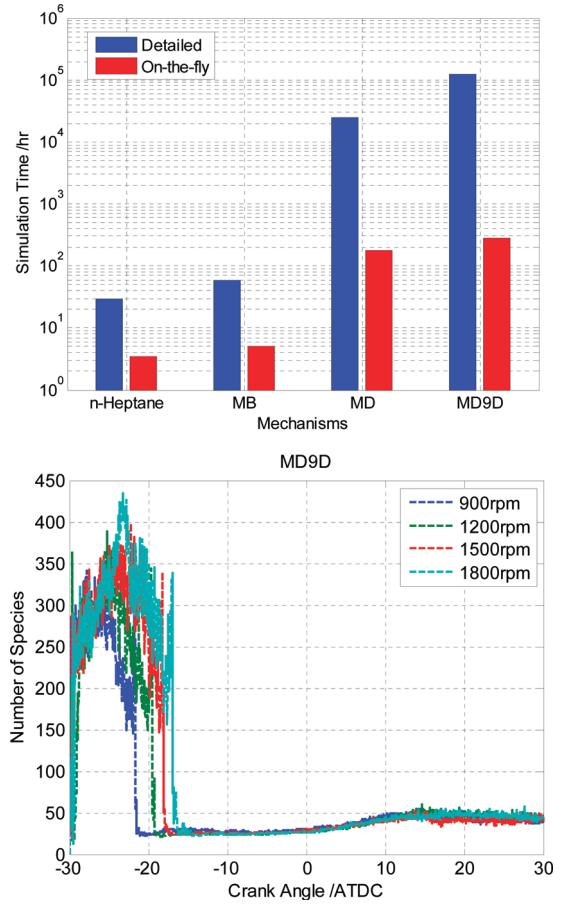

Figure 5. Simulation time reduction for different fuels (upper figure) and mechanism reduction for methyl-9-decenoate (lower figure).

reduction for all the four mechanisms with on-the-fly is quite significant. Time needed for the two small mechanism simulations is reduced by more than 90% with on-the-fly reduction. For the two large mechanisms MD and MD9D, the computational time required using the on-the-fly reduction is reduced by several orders of magnitude (approximately 200−300 h) compared with the estimated simulation time with detailed mechanisms, which is hundreds of days on the basis of the time it takes for the first several computational cycles. The size of reduced mechanisms throughout the simulation is also much smaller compared to the detailed mechanism. For example in the MD9D simulation (Figure 5), the largest reduced mechanism during the simulation is only over 400 species, about only 12% of the total number of species in the detailed mechanism. The simulation with MD mechanism also has similar ratio between reduced mechanisms and detailed mechanism. Therefore, on-the-fly reduction is a powerful and efficient mechanism simplification tool that

dx.doi.org/10.1021/ef2019512 | Energy Fuels 2012, 26, 976−983

enables us to incorporate large chemistry networks in the engine CFD simulations.

Combustion Characteristics Based on HCCI Engine Simulation. One of the most important combustion characteristics is the ignition timing. In Figure 6, we compare the ignition

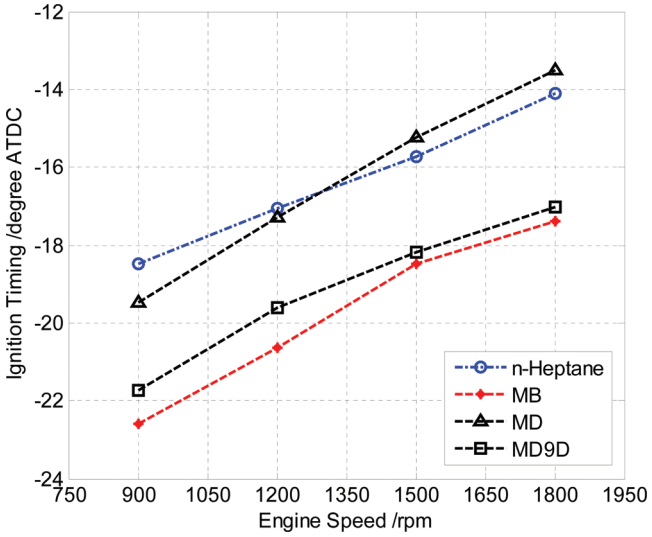

Figure 6. Ignition timing for different fuels in HCCI engine simulations.

timing in terms of crank angle for the four considered fuels under HCCI engine condition obtained in KIVA simulations. As shown in the figure, the ignition timing of MB and MD9D is apparently earlier than that of the hydrocarbon fuel *n*-heptane by two to three crank angle degrees, while MD shows comparable ignition timing to *n*-heptane. These results appropriately reflect the reactivity of these fuels, as reported in the literature. In general, biodiesel fuel is considered to have higher cetane number, that is, earlier ignition timing. As reported in the study by Freedman et al.,[42] cetane number of methyl esters increases as the carbon chain length becomes longer. The cetane number of MD reported in their study was 47.9, compared with cetane number 56 for *n*-heptane reported in ref 43. Therefore, our simulation results demonstrate the relatively higher reactivity for biodiesel fuels, while the similar reactivity of MD and *n*-heptane is also consistent with their comparable cetane numbers.

It should also be observed from Figure 6 that, as engine speed increases, the ignition timing for all the tested fuel is delayed. As engine speed increases, the actual reaction rate in terms of absolute time does not necessarily change, but the piston is moving sufficiently faster relative to the rates of chemical reactions.[44] Therefore, at higher engine speed, the same reaction progress will occur at a later crank angle, which is observed as retarded ignition timing in terms of crank angle degrees.

In addition to the ignition timing study, we also successfully captured the early formation of CO and CO_2 in biodiesel combustion process. The early formation of CO and CO_2 is experimentally observed in the studies of rapeseed oil methyl ester oxidation.[45] Herbinet et al. reports that CO and CO_2 formation is mainly due to the oxidation of the ester groups before the main ignition, in which one of the oxygen atoms in the produced CO_2 is contributed by the ester group via OCHO radical.[14] In our simulation, the early formation of CO and CO_2 of oxygenated biodiesel surrogates is successfully captured, as shown in Figure 7,

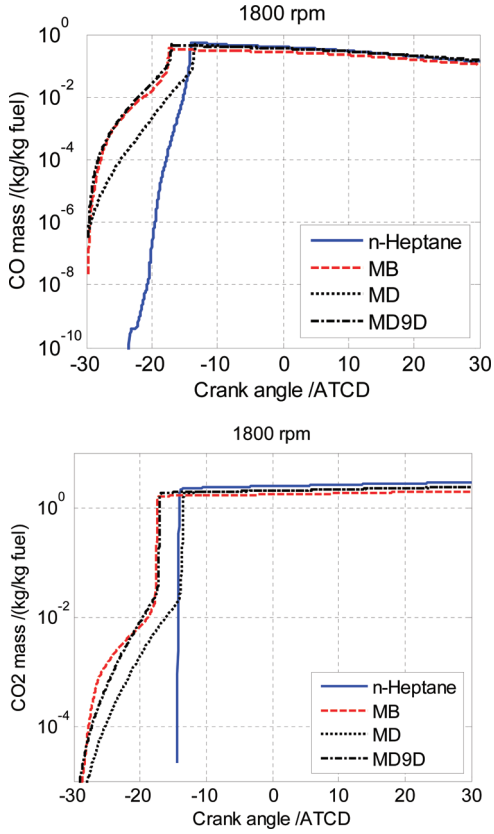

Figure 7. Early formation of CO and CO_2 for biodiesel fuels compared with *n*-heptane.

compared with *n*-heptane, which does not exhibit such phenomena due to its hydrocarbon molecular structure.

CO and NO Emissions. To evaluate the emission features of different types of fuels, CO and NO emissions are calculated and compared at different engine speeds for each fuel, as shown in Figures 8 and 9.

In the literature, CO emission of biodiesel fuels reported in most studies[8] is reduced compared to that of conventional fuels. The oxygenated feature of biodiesel fuels is widely considered as the reason for lower CO emissions because the presence of extra oxygen in the molecule results in more complete combustion possible. This is also reflected in our HCCI engine simulation results, shown in Figure 8. CO emission of MB at different engine speeds is apparently lower than that of the other fuels because it has the highest oxygen content in the molecule. For the two larger biodiesel mechanisms MD and MD9D, which have oxygen content lower than MB but higher than *n*-heptane, the CO emissions are correspondingly higher than in the case of MB and lower than in the case of *n*-heptane. *n*-Heptane with no oxygen in the molecule has the highest CO emission among the tested fuels. These results consistently show the trend that biodiesel has the potential to reduce CO emission as a result of its oxygenated chemical structure. On the other hand, we can observe from Figure 8, as well, that different CO emissions for these fuels are also related with their different cetane numbers, that is, different reactivity. The higher the cetane number is, the faster the reaction completion is, and thus, the lower the probability to form fuel-rich regions, which are usually related to CO emissions. For instance, although MD and MD9D have similar oxygen content, the faster ignition of MD9D leads to an overall lower CO emission compared to that

dx.doi.org/10.1021/ef2019512 | *Energy Fuels* 2012, 26, 976–983

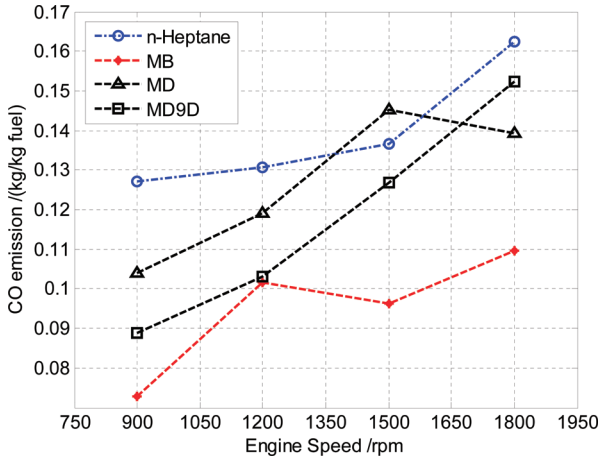

Figure 8. CO emissions for different fuels at different engine speeds.

of MD. Therefore, both oxygenation and advanced ignition contribute to the lower CO emissions.

Besides, we observed that CO emission increases for all the tested fuels as engine speed increases. This result can be due to the retarded ignition and slower kinetic processes relative to piston movement at higher engine speed, which leads to less actual time for chemical reactions to complete.

By using nitrogen-flux analysis with NO_x formation chemistry, we are also able to capture NO emissions of different types of fuels. NO emission is highly related to temperature.[4,10] The higher the temperature is, the more NO is formed. In the literature, different trends of biodiesel NO_x emissions compared with conventional fuels have been reported. Most studies found higher NO emission under diesel engine conditions[8] because faster ignition after fuel injection could result in higher peak temperature in the cylinder. However, this is not usually the case under HCCI engine conditions. In the HCCI engine, ignition does not necessarily occur at around top dead center (TDC) as is the case in compression and spark ignition engines. Therefore, we do not observe a distinct correlation between peak temperature and NO emission level in our results. Instead, NO emission is most likely to be related with the overall in-cylinder temperature, as a result of the different fuel heating values.

In Figure 9, NO emissions for each fuel obtained in the HCCI engine simulations are compared. As described in the figure, NO emission predicted with the three biodiesel surrogates mechanisms is less than that predicted by *n*-heptane mechanism. The lower NO emission could be due to the lower heating value of biodiesel fuels, which is reflected by the total heat release data shown in Figure 10. Lower heating value decreases the overall in-cylinder temperature that can possibly be reached and thus reduces NO formation.

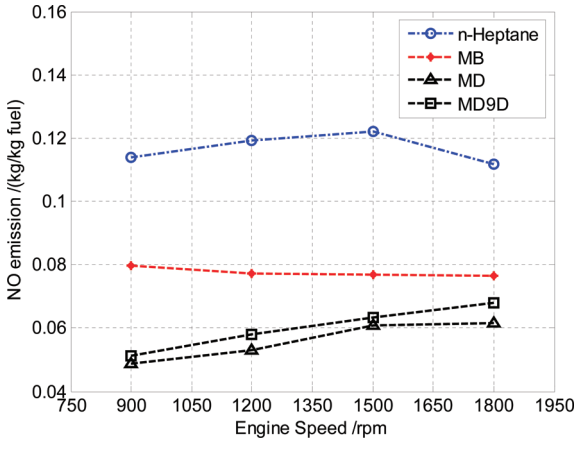

Figure 9. NO emissions for different fuels at different engine speeds.

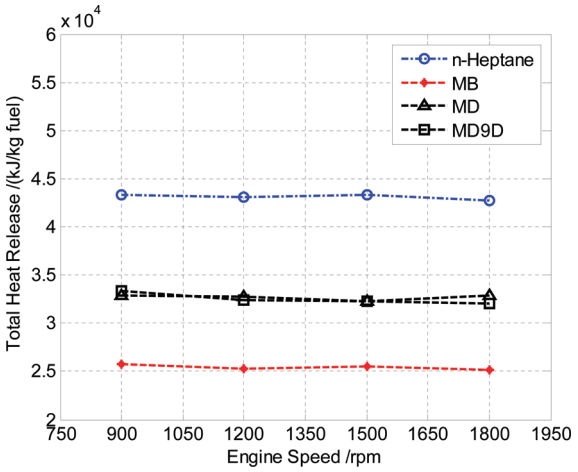

Figure 10. Total heat release for different fuels at different engine speeds.

Another feature we can observe from Figure 9 is that MB generates higher NO emission than the other two biodiesel surrogates. This phenomenon could be explained by the fact that NO emission is also connected with fuel-air ratio during the combustion process. As pointed out by Um et al.[4] in their numerical study of an HCCI engine fueled with biodiesel, high NO emission is likely to occur under fuel lean conditions where fuel oxidation tends to be more complete. Because the small surrogate MB has about 31% oxygen content by molecular weight, which is much higher than about 17% for MD and MD9D, it can reach more complete fuel oxidation than the two large biodiesel surrogates, giving birth to more possible fuel lean regions in the cylinder and thus higher NO formation.

Engine Performance. The calculated engine performance parameters are shown in Figure 11, including work done per cycle and the power output at different engine speeds for each fuel. It is found that the three biodiesel surrogates produce less work per engine cycle and correspondingly less engine power output compared to *n*-heptane. This energy production trend is also consistent with the observation illustrated in Figure 10 that biodiesel has lower total heat release, or heating value, than conventional diesel.

However, if we focus on the two large biodiesel surrogates MD and MD9D, we can see from Figures 10 and 11 that although similar amount of total heat release is observed, they still produce different level of engine power output. To understand this, we also need to take into account the different ignition timing of the two fuels (see Figure 6). Because at all the considered engine speeds MD9D exhibits advanced ignition compared to MD, the in-cylinder pressure in MD9D combustion increases earlier than that in MD combustion. According to eq 4, work done by the engine is reflected by the integration area under the $p-V$ curve. Because the volume change is negative during the compression stroke, the engine has to perform more negative work in MD9D combustion, which lowers the overall work done during the entire engine cycle and, accordingly, leads to less engine power output. Although

dx.doi.org/10.1021/ef2019512 | *Energy Fuels* 2012, 26, 976–983

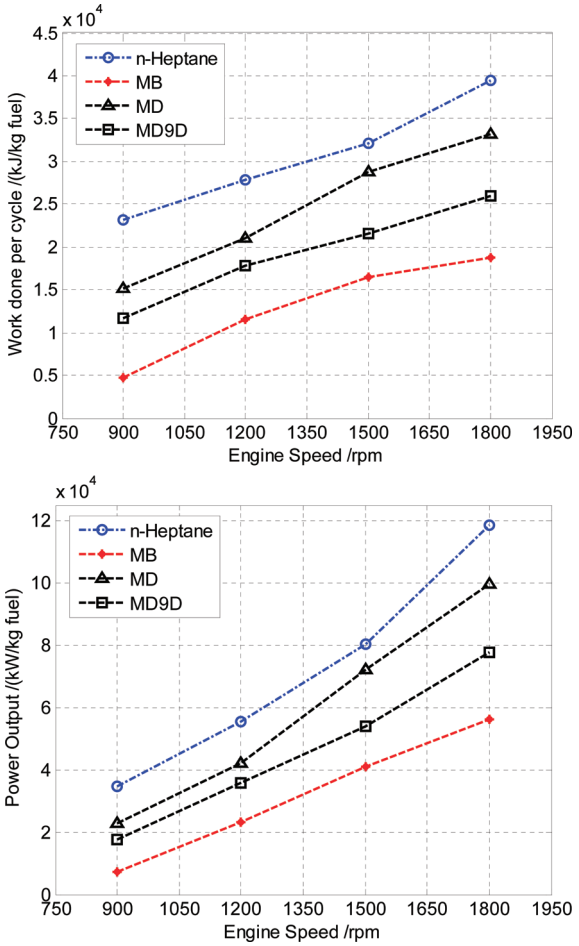

Figure 11. Work done per cycle and power output for different fuels at different engine speeds.

MD9D has similar total heat release during the engine cycle, a larger portion of the released energy is used to overcome the compression resistance, and thus, less energy is left to output engine power.

For the same reason, we can also observe from Figure 11 that, for each fuel, as engine speed increases, the overall power output is also increasing because the delayed ignition timing at higher engine speeds reduces the negative work done in the compression stroke, although the total heat release maintains almost the same level at different engine speeds.

The above discussion reveals that the power output in the HCCI engine is related to both the heating value and the ignition timing of the fuel. For biodiesel, with advanced ignition timing and lower heating value, the power output under HCCI engine conditions is less than that of the conventional diesel fuels.

CONCLUSIONS

In this work, two detailed mechanisms for large biodiesel surrogates are incorporated in the multidimensional CFD for the first time with on-the-fly reduction technique. The engine simulation with these large mechanisms is enabled by reducing the computational time to an acceptable range. The size of mechanism used in the chemistry calculation in our study is also significantly reduced, while still maintaining reliable accuracy. Important combustion characteristics, emission features, and engine performance of biodiesel are successfully captured and compared with conventional diesel fuels under HCCI engine conditions. The fuel comparison suggests that biodiesel has more advanced ignition timing than conventional diesel fuels under various conditions. It is also observed that biodiesel generates lower CO and NO emissions due to its oxygenation and lower heating value. The work done and engine power output for biodiesel fuels are also found to be lower due to lower heating value and advanced ignition timing. These engine simulations can provide important insight to study the chemical characteristics of biodiesel and its impact on the engine design and operation.

It is also realized from our study that the on-the-fly reduction is a powerful tool to simplify detailed chemistry in realistic reactive flow simulations. With the capacity of reducing computational intensity and mechanism complexity, we can have the confidence to employ our integrated KIVA/on-the-fly reduction framework to more realistic flow models and more complicated biodiesel kinetic mechanisms.

Although on-the-fly reduction greatly reduces the computational costs, KIVA simulations with large biodiesel mechanisms still take a relatively long time at approximately 200 to 300 h with our Dell T7500 workstation. Also, despite the mechanism reduction for chemistry calculation, the full species set is still involved to handle transport. In practical or industrial applications, transport of thousands of species is extremely unaffordable. Therefore, we still need to focus on the integration of both global and dynamic reduction approaches to further facilitate the accommodation of larger detailed chemical kinetic mechanisms in reactive flow simulations.

AUTHOR INFORMATION

Corresponding Author

*Tel: 1 (732) 445-2971. Fax: 1 (732) 445-2581. E-mail: marianth@soemail.rutgers.edu.

Notes

The authors declare no competing financial interest.

ACKNOWLEDGMENTS

The authors gratefully acknowledge financial support from NSF CBET Grant No. 0730582 and ONR contract N0014-10-10440.

REFERENCES

(1) Basha, S. A.; Gopal, K. R.; Jebaraj, S. A review on biodiesel production, combustion, emissions, and performance. *Renewable Sustainable Energy Rev.* **2009**, *13* (6−7), 1628−1634.

(2) Ayhan, D. Importance of biodiesel as transportation fuel. *Energy Policy* **2007**, *35* (9), 4661−4670.

(3) Sharma, Y. C.; Singh, B.; Upadhyay, S. N. Advancements in development and characterization of biodiesel: A review. *Fuel* **2008**, *87* (12), 2355−2373.

(4) Um, S.; Park, S. W. Numerical study on combustion and emission characteristics of homogeneous charge compression ignition engines fueled with biodiesel. *Energy Fuels* **2010**, *24* (2), 916−927.

(5) Herbinet, O.; Pitz, W. J.; Westbrook, C. K. Detailed chemical kinetic mechanism for the oxidation of biodiesel fuels blend surrogate. *Combust. Flame* **2010**, *157* (5), 893−908.

(6) Pitz, W. J.; Mueller, C. J. Recent progress in the development of diesel surrogate fuels. *Prog. Energy Combust. Sci.* **2011**, *37* (3), 330−350.

(7) Zhu, L.; Cheung, C. S.; Zhang, W. G.; Huang, Z. Combustion, performance and emission characteristics of a DI diesel engine fueled with ethanol−biodiesel blends. *Fuel* **2011**, *90* (5), 1743−1750.

(8) Lapuerta, M.; Armas, O.; Rodríguez-Fernández, J. Effect of biodiesel fuels on diesel engine emissions. *Prog. Energy Combust. Sci.* **2008**, *34* (2), 198−223.
(9) Lee, C. S.; Park, S. W.; Kwon, S. I. An experimental study on the atomization and combustion characteristics of biodiesel-blended fuels. *Energy Fuels* **2005**, *19* (5), 2201−2208.
(10) Brakora, J. L.; Reitz, R. D. Investigation of NO_x predictions from biodiesel-fueled HCCI engine simulations using a reduced kinetic mechanism. *SAE Technical Paper Series* **2010**, 2010−010577.
(11) Lai, J. Y. W.; Lin, K. C.; Violi, A. Biodiesel combustion: Advances in chemical kinetic modeling. *Prog. Energy Combust. Sci.* **2011**, *37* (1), 1−14.
(12) Fisher, E. M.; Pitz, W. J.; Curran, H. J.; Westbrook, C. K. Detailed chemical kinetic mechanisms for combustion of oxygenated fuels. *Proc. Combust. Inst.* **2000**, *28* (2), 1579−1586.
(13) Um, S.; Park, S. W. Modeling effect of the biodiesel mixing ratio on combustion and emission characteristics using a reduced mechanism of methyl butanoate. *Fuel* **2010**, *89* (7), 1415−1421.
(14) Herbinet, O.; Pitz, W. J.; Westbrook, C. K. Detailed chemical kinetic oxidation mechanism for a biodiesel surrogate. *Combust. Flame* **2008**, *154* (3), 507−528.
(15) Naik, C.; Westbrook, C. K.; Herbinet, O.; Pitz, W. J.; Mehl, M. Detailed chemical kinetic reaction mechanism for biodiesel components methyl stearate and methyl oleate. *Proceedings of the 33rd International Symposium on Combustion*, Beijing, China, 1−6 Aug 2010.
(16) Lu, T.; Law, C. K. Toward accommodating realistic fuel chemistry in large-scale computations. *Prog. Energy Combust. Sci.* **2009**, *35* (2), 192−215.
(17) Androulakis, I. P. Kinetic mechanism reduction based on an integer programming approach. *AIChE J.* **2000**, *46* (2), 361−371.
(18) Bhattacharjee, B.; Schwer, D. A.; Barton, P. I.; Green, W. H. Optimally-reduced kinetic models: Reaction elimination in large-scale kinetic mechanisms. *Combust. Flame* **2003**, *135* (3), 191−208.
(19) Petzold, L.; Zhu, W. Model reduction for chemical kinetics: An optimization approach. *AIChE J.* **1999**, *45* (4), 869−886.
(20) Rabitz, H.; Kramer, M.; Dacol, D. Sensitivity analysis in chemical kinetics. *Ann. Rev. Phys. Chem.* **1983**, *34* (1), 419−461.
(21) Turanyi, T. Reduction of large reaction mechanisms. *New J. Chem.* **1990**, *14* (11), 795−803.
(22) Wei, J.; Kuo, J. C. W. Lumping analysis in monomolecular reaction systems. analysis of the exactly lumpable system. *Ind. Eng. Chem. Fundam.* **1969**, *8* (1), 114−123.
(23) Androulakis, I. P.; Grenda, J. M.; Bozzelli, J. W. Time-integrated pointers for enabling the analysis of detailed reaction mechanisms. *AIChE J.* **2004**, *50* (11), 2956−2970.
(24) Pope, S. B. Computationally efficient implementation of combustion chemistry using in situ adaptive tabulation. *Combust. Theory Modell.* **1997**, *1* (1), 41−63.
(25) Banerjee, I.; Ierapetritou, M. G. An adaptive reduction scheme to model reactive flow. *Combust. Flame* **2006**, *144* (3), 619−633.
(26) Lu, T.; Law, C. K. A directed relation graph method for mechanism reduction. *Proc. Combust. Inst.* **2005**, *30* (1), 1333−1341.
(27) He, K.; Ierapetritou, M. G.; Androulakis, I. P. A graph-based approach to developing adaptive representations of complex reaction mechanisms. *Combust. Flame* **2008**, *155* (4), 585−604.
(28) Turanyi, T.; Tomlin, A. S.; Pilling, M. J. On the error of the quasi-steady-state approximation. *J. Phys. Chem.* **1993**, *97* (1), 163−172.
(29) Chen, J. Y. A General procedure for constructing reduced reaction mechanisms with given independent relations. *Combust. Sci. Technol.* **1988**, *57* (1−3), 89−94.
(30) Maas, U.; Pope, S. B. Simplifying chemical kinetics: Intrinsic low-dimensional manifolds in composition space. *Combust. Flame* **1992**, *88* (3−4), 239−264.
(31) Lam, S. H.; Goussis, D. A. The CSP method for simplifying kinetics. *Int. J. Chem. Kinetics* **1994**, *26* (4), 461−486.
(32) Lu, T.; Ju, Y.; Law, C. K. Complex CSP for chemistry reduction and analysis. *Combust. Flame* **2001**, *126* (1−2), 1445−1455.
(33) Whitehouse, L. E.; Tomlin, A. S.; Pilling, M. J. Systematic reduction of complex tropospheric chemical mechanisms. Part II: Lumping using a time-scale based approach. *Atmos. Chem. Phys.* **2004**, *4* (7), 2057−2081.
(34) He, K.; Androulakis, I. P.; Ierapetritou, M. G. On-the-fly reduction of kinetic mechanisms using element flux analysis. *Chem. Eng. Sci.* **2010**, *65* (3), 1173−1184.
(35) Revel, J.; Boettner, J. C.; Cathonnet, M.; Bachman, J. S. Derivation of a global chemical kinetic mechanism for methane ignition and combustion. *J. Chim. Phys. Phys.—Chim. Biol.* **1994**, *91*, 365−382.
(36) Curran, H. J.; Gaffuri, P.; Pitz, W. J.; Westbrook, C. K. A comprehensive modeling study of *n*-heptane oxidation. *Combust. Flame* **1998**, *114* (1−2), 149−177.
(37) Amsden, A. A. *KIVA-3V: A Block-Structured KIVA Program for Engines with Vertical or Canted Valves*, LA-13313-MS; Los Alamos National Laboratory: Los Alamos, NM, 1997.
(38) Kee, R. J.; RupleyF. M., Meeks, E.; Miller, J. A. *CHEMKIN-III: A FORTRAN Chemical Kinetics Package for the Analysis of Gas-Phase Chemical and Plasma Kinetics*; Sandia National Labs: Livermore, CA, 1996.
(39) He, K.; Ierapetritou, M. G.; Androulakis, I. P. Integration of on-the-fly kinetic reduction with multidimensional CFD. *AIChE J.* **2009**, *56* (5), 1305−1314.
(40) He, K.; Androulakis, I. P.; Ierapetritou, M. G. Multi-element flux analysis for the incorporation of detailed kinetic mechanisms in reactive simulations. *Energy Fuels* **2009**, *24* (1), 309−317.
(41) Heywood, J. B. *Internal Combustion Engine Fundamentals*; McGraw-Hill: New York, 1988.
(42) Freedman, B.; Bagby, M. Predicting cetane numbers of *n*-alcohols and methyl esters from their physical properties. *J. Am. Oil Chem. Soc.* **1990**, *67* (9), 565−571.
(43) Lü, X.; Ji, L.; Zu, L.; Hou, Y.; Huang, C.; Huang, Z. Experimental study and chemical analysis of *n*-heptane homogeneous charge compression ignition combustion with port injection of reaction inhibitors. *Combust. Flame* **2007**, *149* (3), 261−270.
(44) Kelly-Zion, P. L.; Dec, J. E. A computational study of the effect of fuel type on ignition time in homogenous charge compression ignition engines. *Proc. Combust. Inst.* **2000**, *28* (1), 1187−1194.
(45) Dagaut, P.; Gail, S.; Sahasrabudhe, M. Rapeseed oil methyl ester oxidation over extended ranges of pressure, temperature, and equivalence ratio: Experimental and modeling kinetic study. *Proc. Combust. Inst.* **2007**, *31* (2), 2955−2961.